p-ISSN 2089 – 0133 e-ISSN 2477-6416
URL : https://jurnal.uns.ac.id/ijap/article/view/8331
Indonesian Journal of Applied Physics (IJAP) Vol. 14 No. 2 page 290
DOI : https://doi.org/10.13057/ijap.v14i2.83371

REDUCED GRAPHENE OXIDE/SIO_2 BASED ELECTRODE MATERIAL: SYNTHESIS AND CHARACTERIZATION

Sinta Nur Mazida Rafiq[1], Dina Rahmawati[1], Mukhtar Effendi[1], Sib Krishna Ghoshal[2], Candra Kurniawan[3], Wahyu Widanarto*[1]

[1] Department of Physics, Universitas Jenderal Soedirman, Purwokerto, Indonesia
[2] Department of Physics and Laser Centre, AMORG, Faculty of Science, Universiti Teknologi Malaysia, Johor Bahru, Skudai, Malaysia
[3] Research Center for Advanced Materials, BRIN, Tangerang, Indonesia
* wahyu.widanarto@unsoed.ac.id

Received 15-01-2024, Revised 05-04-2024, Accepted 03-07-2024,
Available Online 03-07-2024, Published Regularly October 2024

ABSTRACT

Developing a Reduced Graphene Oxide (rGO) synthesis method based on rice husk as a composite electrode material with Silica (SiO_2) has garnered particular attention for designing high-quality electrode materials. This research successfully synthesized rGO/SiO_2 material from rice husk-derived activated carbon through a one-step thermal reduction process at 200 °C. This method offers a simple, efficient, cost-effective, and environmentally friendly synthesis approach. The resulting samples' morphology, surface composition, crystal structure, surface area, and pore diameter size were characterized using FE-SEM, EDX, XRD, and SAA-BET. EDX characterization results confirmed the predominance of carbon content in the samples. At the same time, the natural emergence of SiO_2 without external addition due to thermal reduction at 200 °C was an intriguing initial finding. The spherical crystal structure of silica between the wrinkled rGO layers was confirmed through FE-SEM and XRD analysis. The synergistic effect between SiO_2 and rGO significantly increased the sample's surface area, with a value of 34.17 m^2/g for the rGO sample before thermal reduction, which increased to 121.24 m^2/g after the thermal reduction process at 200 °C. This process also positively impacted the reduction in pore size of rGO/SiO_2, with a value decreasing from 9.33 nm before thermal reduction to 4.89 nm after the thermal reduction process. The results of this study demonstrate that rGO/SiO_2 synthesized from rice husk-derived activated carbon holds great potential as a high-performance electrode material, combining the advantages of thermal reduction, natural Si content, and increased surface area for diverse applications.

Keywords: rice husk; carbon; composite; electrode; thermal reduction.

Cite this as: Rafiq, S. N. M., Rahmawati, D., Effendi, M., Ghoshal, S. K., Kurniawan, C., & Widanarto, W. 2024. Reduced Graphene Oxide/SiO_2 Based Electrode Material: Synthesis and Characterization. *IJAP: Indonesian Journal of Applied Physics, 14*(2), 290-300. doi: https://doi.org/10.13057/ijap.v14i2.83371

INTRODUCTION

The naturally occurring two-dimensional (2D) material known as graphene possesses carbon atoms that are sp2-hybridized, forming a honeycomb crystal lattice [1]. Graphene exhibits remarkable properties, such as high electrical conductivity and mobility, a large specific surface area, and excellent thermal conductivity, making it an unparalleled candidate for various innovative applications [2–4]. Furthermore, numerous studies have demonstrated the potential of graphene and graphene-like materials in practical applications like sensors, batteries, and supercapacitors [4–8]. However, despite the increasing demand from various

industries, the availability of graphene remains limited, and large-scale production of high-quality graphene remains a significant challenge [9–11]. Various synthesis methods are continuously being developed, and recently, chemical synthesis methods have made it possible to produce graphene in large quantities with customizable properties designed to meet specific application needs. The most commonly used chemical method involves the reduction of graphene oxide [12–14].

Reduced Graphene Oxide (rGO) is essential in developing energy storage technologies. A standard method for producing rGO involves the conversion of graphite into graphene oxide (GO), followed by the exfoliation of layers to achieve GO. A reducing agent decreases the number of oxide bonds in GO [15]. However, this method has several limitations, including hazardous chemicals, a complex synthesis route, and the need for high temperatures for an extended period, making it an expensive process. Therefore, there is an urgent need to develop a more straightforward, environmentally friendly, cost-effective, and sustainable method for commercial-scale graphene production. Recent research indicates that biomass such as peanut shells, palm oil waste, wood sawdust, rice husks, and coconut shells can serve as potential resources for producing graphene-like materials economically [16–19]. Biomass, an abundant, economical, and underutilized source of green waste rich in carbon, can easily be harnessed to create derivative graphene materials [20]. However, graphene derived from activated carbon from biomass often exhibits lower electrical conductivity than pure graphite or graphene [21]. It is attributed to impurities and defects within the resulting rGO structure. Various methods were proposed to address this weakness. One of the methods involves compositing rGO with SiO_2 to enhance its electrical conductivity, particularly in energy storage applications. Nonetheless, mixing and synthesizing rGO/SiO_2 composites can become more intricate and necessitate specialized technologies, adding complexity to production and associated costs.

The synthesis of rGO using rice husk as a raw material allows for the fabrication of rGO/SiO_2 composites with precise temperature control. SiO_2 can naturally be found in rice husk components and other organic materials [22,23]. However, a heating processing step is often required to obtain purer or higher SiO_2 concentrations. The synthesis of rGO/SiO_2 based on rice husk was conducted with variations in heating at temperatures of 0, 100, 200, and 300 °C. The resulting samples' morphology, composition, crystal structure, surface area, and pore diameter were analyzed using FE-SEM, EDX, XRD, and SAA-BET techniques. This method offers a simple, efficient, cost-effective, and environmentally friendly synthesis approach.

EXPERIMENTAL PROCEDURE

Preparation of rGO

The rice husks (purchased from a local market in Indonesia) were cleaned with water and oven-dried at 110 °C for 3 hours using this technique. The dried rice husks were then carbonized for an hour in an electric furnace (300 °C) to make charcoal. The charcoal was then activated for 24 hours by potassium hydroxide or caustic potash (KOH, 5 Mol), with a charcoal to KOH ratio of 1:4. After that, the activated charcoal was filtered with hydrochloric acid (HCl, 0.1 Mol) and distilled water until the pH was neutrally flowed, followed by 6 hours of oven drying at 100 °C. Finally, rGO was produced by milling 10 g of the resulting activated charcoal for 50 minutes [24-27].

Preparation of Reduced Graphene Oxide/SiO_2

rGO/SiO_2 material is synthesized in a one-step process through thermal reduction. Initially, rGO is formed and then subjected to thermal reduction at 200°C for 30 minutes using a muffle

furnace. The obtained rGO samples were labelled rGO-200. Additional rGO samples were prepared under different reduction conditions: rGO-0 (no thermal reduction), rGO-100 (reduced at 100 °C), and rGO-300 (reduced at 300 °C) to facilitate comparison. This method offers a simple, efficient, cost-effective, and environmentally friendly synthesis approach, as illustrated in Figure 1, which shows the preparation steps.

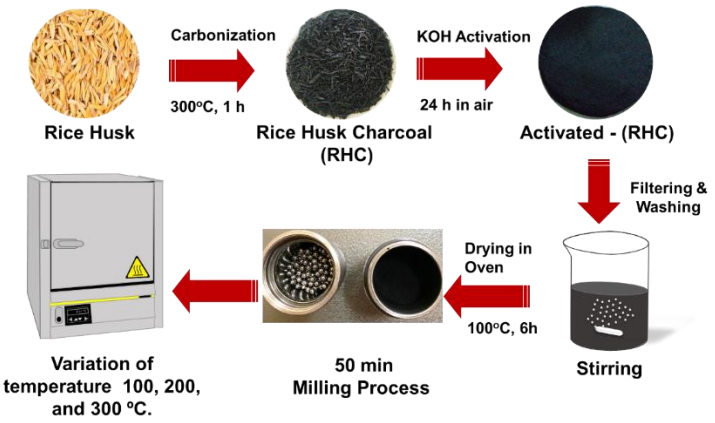

Figure 1. Illustration of rGO/SiO_2 sample preparation steps

Characterizations of Reduced Graphene Oxide/SiO_2

The as-synthesized rGO and rGO/SiO_2 were characterized using different techniques. The surface morphology, microstructure, and constituent elements of the prepared rGOs were examined using the field-emission scanning electron microscope (FE-SEM, JEOL) attached with an energy-dispersive X-ray spectrometer (EDX). The crystal structures and phases of the rGOs were examined using a Rigaku-SmartLab (3 kW) X-ray diffractometer equipped with the Cu-Kα line of wavelength (λ) ≈ 0.1541874 nm. The Surface Area Analyzer (SAA Quantachrome Instrument Version 11.03) was used to determine the specific surface area and pores size distribution of rGO, wherein Brunauer, Emmett, and Teller (BET) and Barret Joyner Hallenda (BJH) models were utilized.

RESULTS AND DISCUSSION

Diffraction Pattern of Reduced Graphene Oxide

Based on the diffractogram analysis, the produced rGO exhibits two distinguishable phases: amorphous and crystalline. The qualitative differences between these two phases are observable through the characteristic shape of the diffraction peaks in the X-ray diffraction (XRD) pattern. Crystalline phases are typically characterized by sharp diffraction peaks, which are localized at specific positions in the spectrum. These well-defined peaks unequivocally indicate atoms or molecules ordered and organized arrangement within a crystal lattice structure. On the other hand, the amorphous phase is characterized by broad diffraction peaks, implying structural irregularity within the material. The XRD pattern in Figure 2 reveals the distinctive features of the formed sample, with sharp peaks identifying the crystalline phase and broad peaks depicting the characteristics of the amorphous phase.

The rGO-0 samples exhibit an amorphous diffraction pattern with weak diffraction peaks observed at positions of 2θ around 25° and 35.7° before undergoing thermal reduction. It consistently can be attributed to the graphite oxide (GO) structure [28]. Following the reduction process at 100 °C (rGO-100), the sample slightly shifts in diffraction peaks towards lower angles. This shift indicates a change in the crystal structure or a reduction in defects within the

structure, resulting from decreased oxygen groups bound to the carbon layers. In the rGO-100 sample, amorphous diffraction patterns remained visible, with weak peaks observed at 2θ angles of approximately 24.23° and 35.5°. These findings are consistent with FESEM characterization, which also indicates irregularities in the structure and surface morphology of the sample. Thus, the results of XRD and FESEM characterizations confirm the presence of amorphous elements in the structure and morphology of the sample, providing concrete evidence of the existing disorderly nature.

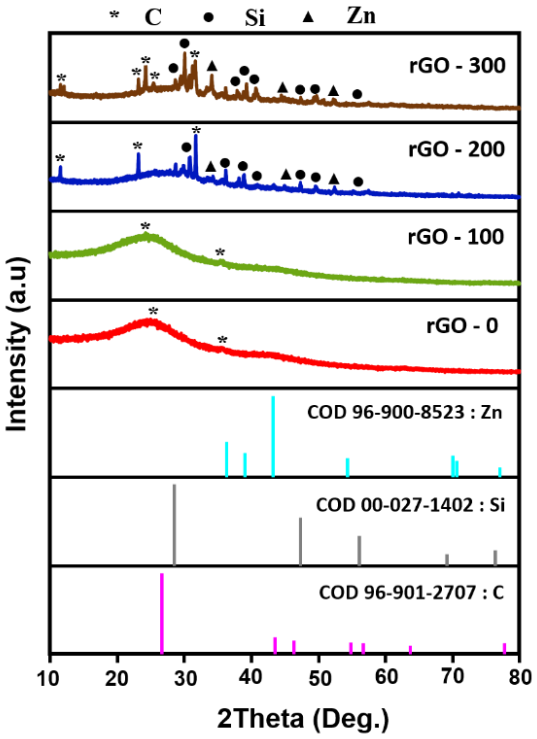

Figure 2. XRD patterns of as-synthesized samples.

A significant difference is observed between the rGO-200 and rGO-300 samples, which are reflected in their crystal structures and are characterized by several sharp diffraction peaks. The crystal structure formation indicates a restructuring process at the atomic and molecular levels, resulting in changes in the structure and composition of these samples. In the rGO-200 sample, sharp diffraction peaks were observed at 26.22°, indicating the presence of a carbon phase. This pattern is similar to the reference in the COD (Crystallography Open Database) file number 96-901-2707. Additionally, a crystalline silica phase naturally emerged and increased during the thermal reduction process at 200 °C. The identification of this silica phase has been confirmed and matches with the available reference pattern (COD File, 00-027-1402). Silica is one of the components in the rGO sample originating from rice husks [22,29]. When the temperature is raised to 200°C, more intense heating can lead to the decomposition or transformation of the SiO_2 contained in rGO. At this temperature, silica may undergo oxidation or structural changes due to the influence of higher heat. This process can result in the degradation or oxidation of the silica in rice husks, which is subsequently detected in the rGO sample. Furthermore, zinc (Zn) content in the rGO sample may be attributed to environmental contamination during production.

Morphology of Reduced Graphene Oxide/SiO_2

Figure 3. illustrates the surface morphology of rGO samples derived from activated rice husk charcoal, processed through reduction at a 15.000-fold image magnification. Observations reveal that most samples exhibit an amorphous morphology characterized by the absence of regular layering. This phenomenon can be attributed to the influence of the milling stage before thermal reduction. The amorphous morphology is most pronounced in the rGO-0 sample, which underwent no reduction process. Meanwhile, in samples heated to 100 °C, there is a discernible albeit not highly significant change in morphology. The resulting structure resembles crumpled tissue balls. It may be attributed to the limited effectiveness of the low-temperature reduction process in achieving a well-ordered crystalline structure in rGO.

After heating at 200 and 300 °C, the samples exhibited variations in Reduced Graphene Oxide (rGO) formed morphology. Some of the samples produced thin sheets of rGO, while others formed crystalline structures resembling the morphology of silica (SiO_2) and zinc (Zn) [29–32]. In the case of the rGO-200 sample, it is evident that the formed Si morphology is situated between the layers of rGO. This variation is likely due to the conditions in which some samples underwent a more effective reduction of graphene oxide. In contrast, others experience the decomposition of organic compounds contained in rice husks. This process resulted in byproducts that can accumulate within the rGO samples.

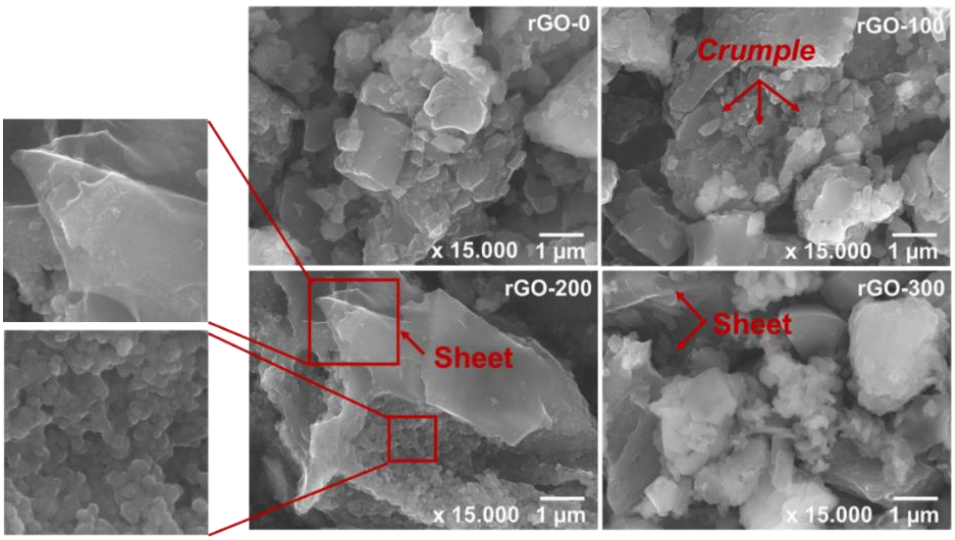

Figure 3. FE-SEM images of the proposed rGO and rGO/SiO_2

Elemental Composition of Reduced Graphene Oxide

Figure 4. depicts the EDX spectrum of an rGO sample, revealing its primary elemental composition, which is predominantly composed of carbon (C), followed by oxygen (O), potassium (K), and SiO_2. Oxygen in this rGO sample is influenced by the carbonization process in an open-air environment. Meanwhile, potassium (K) in rGO can be attributed to the KOH activation and partial washing processes. The origin of SiO_2 in rGO is associated with the natural presence of SiO_2 in rice husks. There is a significant increase in silica content when heating is carried out at 200°C. More detailed information regarding the elemental composition of each sample can be found in Table 1.

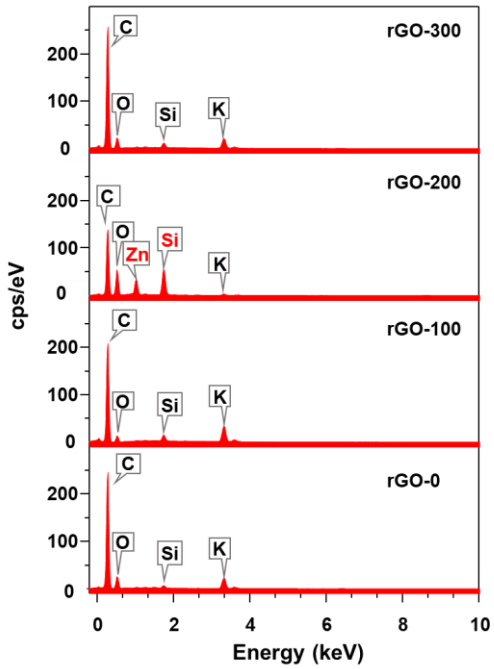

Figure 4. EDX spectra of as-synthesized rGO samples

Table 1. Elemental composition of the studied rGO obtained from EDX analyses

Detected Elements	Samples			
	rGO-0	rGO-100	rGO-200	rGO-300
	atomic%	atomic%	atomic%	atomic%
C	84.0	86.1	74.8	86
O	12.4	8.2	18.8	10.8
K	2.7	4.2	0.3	2.3
Si	0.4	1	3.5	0.7
Zn	0.0	0.0	1.7	0.0
Etc.				

Table 1 shows a 3.5% increase in the Si element in the rGO-200 sample. This increase can be attributed to reduced silanol groups on the silica surface at a temperature of 200 ℃, leading to agglomeration and forming larger silica particles. The increased Si content can impact the resulting pore diameter, with higher Si content leading to smaller pore diameters. Pore diameter size, in turn, affects the specific surface area produced. Higher Si content is associated with more significant specific surface areas [33].

Additionally, a high SiO_2 content in the sample can enhance the conductivity of rGO due to the resulting sheet-like and porous morphology, which provides a continuous conductive path between SiO_2 nanoparticles. It allows for greater electron storage capacity in the sample [32]. However, in the rGO-300 sample, there was a decrease in Si content, possibly resulting from the high reduction temperature, which may have caused some of the Si content to be lost.

Specific Surface Area of Reduced Graphene Oxide

Figure 5 displays a multi-point isothermal BET plot of the as-synthesized rGO samples. The specific surface areas were employed to analyze the diffusion mechanism within the porous

material and to elucidate the selectivity of the catalyst reaction based on the principles of adsorption theory [34,35]. The adsorption isotherms data with relative pressure (*P*/*Po*) values ranging from 0.05 to 0.3 were subjected to the BET equation [36]. The plot of 1/[*W*((*Po*/*P*)-1) against *P*/*Po* showed a linear variation with a correlation coefficient (*r*) of 0.999. Table 2 shows specific surface area values of the rGO samples calculated using the BET method. The surface area of rGO was highest at the thermal reduction of 200 ℃ and then decreased with the increase in reduction temperature. The surface area of rGO is highly dependent on particle size. It reveals that the surface area of rGO is most prominent at a reduction temperature of 200 ℃.

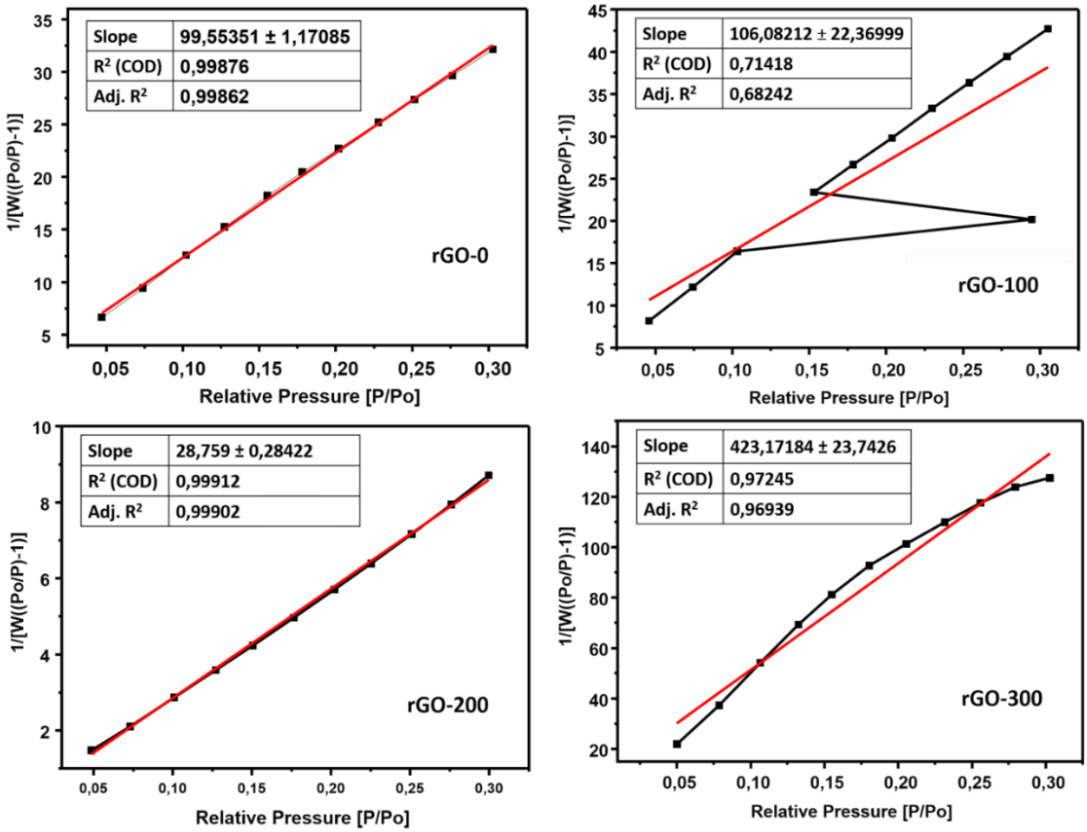

Figure 5. Multiple-point isothermal BET plots of the produced rGO specimens

Table 2 presents comprehensive results on the effect of thermal reduction on surface area and pore diameter. The combination of rGO and SiO2 in the rGO-200 sample significantly increased the surface area from 34.17 m²/g in the rGO sample before thermal reduction to 121.24 m²/g after the thermal reduction process at 200 °C. Additionally, this approach reduced the pore size from 9.33 nm to 4.89 nm.

The rGO sample heated at 200 °C exhibited the highest specific surface area because the heating process at this temperature supports the formation of an optimal rGO structure. Heating at 200 °C effectively reduces the oxygen-functional groups in the GO layers, resulting in a more open graphene structure with increased interlayer spacing, thereby enhancing the specific surface area. Furthermore, the formation of SiO2 within the rGO matrix at this temperature also contributes to the increase in surface area. SiO2 acts as a spacer, maintaining the distance between rGO layers, preventing agglomeration, and ensuring high surface area availability. Thus, heating at 200 °C results in a more open and well-organized rGO structure, supported by the presence of SiO2, leading to the highest specific surface area compared to samples heated at other temperatures.

Table 2. The specific surface area of as-synthesized rGO samples

Sample Code	Specific surface area SBET (m^2/g)	Pore diameter (nm)
rGO-0	34.166	9.329
rGO-100	25.698	10.169
rGO-200	121.244	4.893
rGO-300	8.058	22.920

Figure 6 illustrates the pore size distribution of the prepared rGO samples wherein the results of nitrogen adsorption at 77.35 K were analyzed using the BJH approach. The pores radius in the rGO specimens varied in the range of 1 to 135 nm with sequential peaks around 9.329 (for rGO-0), 10.169 (for rGO-100), 4.893 (for rGO-200), and 22.920 nm (for rGO-300). Moreover, the pore size distribution of rGO samples is dominated in the range of 2 and 50 nm, indicating the formation of a mesoporous structure according to the International Union of Pure and Applied Chemistry (IUPAC) classification scheme. The pore volumes of rGO-0, rGO-100, rGO-200, and rGO-300 were 0.079681, 0.066126, 0.165328, and 0.054904 cm3/g, respectively. In short, the porosity, pore size, and pore volume of the produced rGO were significantly affected by the thermal reduction variation.

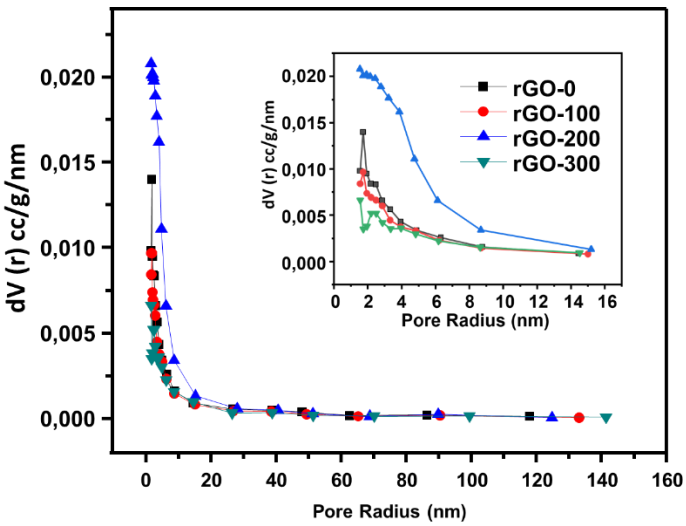

Figure 6. Pores size distribution of rGO specimens obtained from nitrogen adsorption at 77.35 K using the BJH model

CONCLUSION

Reduced Graphene Oxide was successfully produced from rice husk-derived activated carbon through a single-stage thermal reduction process at 200 °C. The natural presence of SiO_2 in this material adds intriguing value. The synthesis method offers a simple, efficient, cost-effective, and environmentally friendly approach. The combination of rGo and SiO_2 significantly increased the sample's surface area, rising from 34.17 m^2/g for rGO before thermal reduction to 121.24 m^2/g after the thermal reduction process at 200 °C. Furthermore, this process has effectively reduced the pore size of rGO/SiO_2, decreasing from 9.33 nm before thermal reduction to 4.89 nm after the process. The results of this study demonstrate that rGO/

SiO_2 derived from activated carbon from rice husk derivatives holds great potential as a high-performance electrode material. This material combines the advantages of thermal reduction, natural SiO_2 content, and enhanced surface area, making it suitable for various applications requiring high-quality electrode materials.

ACKNOWLEDGMENTS

The authors are grateful to Universitas Jenderal Soedirman (Contract number: 27.10/UN23.37/PT.01.03/II/2023) for their financial assistance.

REFERENCES

1 Novoselov, K. S., Geim, A. K., Morozov, S. V., Jiang, D., Zhang, Y., Dubonos, S. V., Grigorieva, I. V., & Firsov, A. A. 2004. Electric field effect in atomically thin carbon films. *Science*, *306*(5696), 666–669.

2 Liu, F., Wang, C., Sui, X., Riaz, M. A., Xu, M., Wei, L., & Chen, Y. 2019. Synthesis of graphene materials by electrochemical exfoliation: Recent progress and future potential. *Carbon Energy*, *1*, 173–199.

3 Nair, R. R., Blake, P., Grigorenko, A. N., Novoselov, K. S., Booth, T. J., Stauber, T., Peres, N. M. R., & Geim, A. K. 2008. Fine structure constant defines visual transparency of graphene. *Science*, *320*(5881), 1308.

4 Mayorov, A. S., Gorbachev, R. V., Morozov, S. V., Britnell, L., Jalil, R., Ponomarenko, L. A., Blake, P., Novoselov, K. S., Watanabe, K., Taniguchi, T., & Geim, A. K. 2011. Micrometer-scale ballistic transport in encapsulated graphene at room temperature. *Nano Letters*, *11*(7), 2396–2399.

5 Yang, W., Ni, M., Ren, X., Tian, Y., Li, N., Su, Y., & Zhang, X. 2015. Graphene in supercapacitor applications. *Current Opinion in Colloid & Interface Science*, *20*(5), 416–428.

6 Ghany, N. A. A., Elsherif, S. A., & Handal, H. T. (2017). Revolution of graphene for different applications: State-of-the-art. *Surfaces and Interfaces*, *9*, 93–106.

7 Salehi-Khojin, A., Estrada, D., Lin, K. Y., Bae, M. H., Xiong, F., Pop, E., & Masel, R. I. 2012. Graphene sensors: Polycrystalline graphene ribbons as chemiresistors. *Advanced Materials*, *24*(52), 52.

8 Liu, J. 2014. Charging graphene for energy. *Nature Nanotechnology*, *9*(10), 739–741.

9 Cheng, Q., Okamoto, Y., Tamura, N., Tsuji, M., Maruyama, S., & Matsuo, Y. 2017. Graphene-like graphite as fast-chargeable and high-capacity anode materials for lithium ion batteries. *Scientific Reports*, *7*, Article 14504.

10 Xu, M., Liang, T., Shi, M., & Chen, H. 2013. Graphene-like two-dimensional materials. *Chemical Reviews*, *113*(5), 3766–3798.

11 Arbuzov, A. A., Muradyan, V. E., & Tarasov, B. P. 2013. Synthesis of graphene-like materials by graphite oxide reduction. *Russian Chemical Bulletin*, *62*, 1962–1966.

12 Bhuyan, Md. S. A., Uddin, Md. N., Islam, Md. M., Bipasha, F. A., Hossain, S. S. 2016. Synthesis of graphene. *International Nano Letters*, *6*, 65–83.

13 Nirmalraj, P. N., Lutz, T., Kumar, S., Duesberg, G. S., & Boland, J. J. 2011. Nanoscale mapping of electrical resistivity and connectivity in graphene strips and networks. *Nano Letters*, *11*(1), 16–22.

14 Xu, B., Yue, S., Sui, Z., Zhang, X., Hou, S., Cao, G., & Yang, Y. 2011. What is the choice for supercapacitors: Graphene or graphene oxide? *Energy & Environmental Science*, *4*(8), 2826.

15 Lavin-Lopez, M. P., Paton-Carrero, A., Sanchez-Silva, L., Valverde, J. L., & Romero, A. 2017. Influence of the reduction strategy in the synthesis of reduced graphene oxide. *Advanced Powder Technology*, *28*, 3195–3203.

16 Purkait, T., Singh, G., Singh, M., Kumar, D., & Dey, R. S. 2017. Large area few-layer graphene with scalable preparation from waste biomass for high-performance supercapacitor. *Scientific Reports*, *7*, Article 15463.

17 Mamat, R. H., Hamzah, F., Hashim, A., Abdullah, S., Alrokayan, S. A. H., Khan, H. A., Safiay, M., Jafar, S. M., Asli, A., Khusaimi, Z., & Rusop, M. 2018. Influence of volume variety of waste cooking palm oil as carbon source on graphene growth through double thermal chemical vapor deposition. In *2018 IEEE International Conference on Semiconductor Electronics (ICSE)* (pp. 53–56). IEEE.

18 Severo, L. S., Rodrigues, J. B., Campanelli, D. A., Pereira, V. M., Menezes, J. W., de Menezes, E. W., Valsecchi, C., Vasconcellos, M. A. Z., Armas, L. E. G. 2021. Synthesis and Raman characterization of wood sawdust ash and wood sawdust ash-derived graphene. *Diamond and Related Materials, 117*, Article 108496.

19 Fahmi, F., Dewayanti, N. A. A., Widiyastuti, W., & Setyawan, H. 2020. Preparation of porous graphene-like material from coconut shell charcoals for supercapacitors. *Cogent Engineering, 7*.

20 Xu, M., Wang, A., Xiang, Y., & Niu, J. 2021. Biomass-based porous carbon/graphene self-assembled composite aerogels for high-rate performance supercapacitor. *Journal of Cleaner Production, 315*, 128110.

21 Sawant, S. A., Patil, A. V., Waikar, M. R., Rasal, A. S., Dhas, S. D., Moholkar, A. V., Vhatkar, R. S., & Sonkawade, R. G. 2022. Advances in chemical and biomass-derived graphene/graphene-like nanomaterials for supercapacitors. *Journal of Energy Storage, 51*, 104445.

22 Ratsameetammajak, N., Autthawong, T., Chairuangsri, T., Kurata, H., Yu, A., & Sarakonsri, T. 2022. Rice husk-derived nano-SiO_2 assembled on reduced graphene oxide distributed on conductive flexible polyaniline frameworks towards high-performance lithium-ion batteries. *RSC Advances, 12*, 14621–14630.

23 Liou, T.-H., Tseng, Y. K., Liu, S.-M., Lin, Y.-T., Wang, S.-Y., & Liu, R.-T. 2021. Green synthesis of mesoporous graphene oxide/silica nanocomposites from rich husk ash: Characterization and adsorption performance. *Environmental Technology & Innovation, 22*, 101424.

24 Mondal, O., Mitra, S., Pal, M., Datta, A., Dhara, S., & Chakravorty, D. 2015. Reduced graphene oxide synthesis by high energy ball milling. *Materials Chemistry and Physics, 161*, 123–129.

25 Dash, P., Dash, T., Rout, T. K., Sahu, A. K., Biswal, S. K., & Mishra, B. K. 2016. Preparation of graphene oxide by dry planetary ball milling process from natural graphite. *RSC Advances, 6*(15), 12657–12668.

26 Mahmoud, A. E. D., Stolle, A., & Stelter, M. 2018. Sustainable synthesis of high-surface-area graphite oxide via dry ball milling. *ACS Sustainable Chemistry & Engineering, 6*(5), 6358–6369.

27 Caicedo, F. M. C., López, E. V., Agarwal, A., Drozd, V., Durygin, A., Hernandez, A. F., & Wang, C. 2020. Synthesis of graphene oxide from graphite by ball milling. *Diamond and Related Materials, 109*, 108064.

28 Benzait, Z., Chen, P., & Trabzon, L. 2021. Enhanced synthesis method of graphene oxide. *Nanoscale Advances, 3*, 223–230.

29 Sekar, S., Aqueel Ahmed, A. T., Inamdar, A. I., Lee, Y., Im, H., Kim, D. Y., & Lee, S. 2019. Activated carbon-decorated spherical silicon nanocrystal composites synchronously-derived from rice husks for anodic source of lithium-ion battery. *Nanomaterials, 9*, 1055.

30 Ma, Y., Di, H., Yu, Z., Liang, L., Lv, L., Pan, Y., Zhang, Y., & Yin, D. 2016. Fabrication of silica-decorated graphene oxide nanohybrids and the properties of composite epoxy coatings research. *Applied Surface Science, 360*, 936–945.

31 Liou, T.-H., & Wang, P.-Y. 2020. Utilization of rice husk wastes in synthesis of graphene oxide-based carbonaceous nanocomposites. *Waste Management, 108*, 51–61.

32 Jiao, L.-S., Liu, J.-Y., Li, H.-Y., Wu, T.-S., Li, F., Wang, H.-Y., & Niu, L. 2016. Facile synthesis of reduced graphene oxide-porous silicon composite as superior anode material for lithium-ion battery anodes. *Journal of Power Sources, 315*, 9–15.

33 Kohli, K., Prajapati, R., Maity, S. K., & Sharma, B. K. 2020. Effect of silica, activated carbon, and alumina supports on NiMo catalysts for residue upgrading. *Energies, 13*, 4967.

34 Widanarto, W., Irma, S., Krishna, S., Kurniawan, C., Handoko, E., & Alaydrus, M. 2022. Improved microwave absorption traits of coconut shells-derived activated carbon. *Diamond and Related Materials, 126*, 109059.

35 Widanarto, W., Romdhony, F., Cahyanto, W. T., Sari, K., Ghoshal, S. K., & Kurniawan, C. 2023. Production of reduced graphene oxide from activated rice husk charcoal using a high-energy ball milling method. *Physica Scripta*, *98*(10), 105902.
36 Widanarto, W., Wulandari, R., Rahmawati, D., Cahyanto, W. T., Sari, K., Effendi, M., ... & Kurniawan, C. 2024. Microwave irradiation-induced yield enhancement of coconut shell biomass-derived graphene-like material. *Physica Scripta*.